Published in final edited form as:
Nat Neurosci. 2010 December ; 13(12): 1472–1480. doi:10.1038/nn.2686.

Yy1 as a molecular link between neuregulin and transcriptional modulation of peripheral myelination

Ye He[1], **Jin Young Kim**[1], **Jeffrey Dupree**[2], **Ambika Tewari**[3], **Carmen Melendez-Vasquez**[3], **John Svaren**[4], and **Patrizia Casaccia**[1]

[1]Department of Neuroscience and Genetics and Genomics, Mount Sinai School of Medicine, New York, New York, USA

[2]Department of Anatomy and Neurobiology, Virginia Commonwealth University, Richmond, Virginia, USA

[3]Department of Cell Biology, Hunter College, New York, New York, USA

[4]Department of Comparative Biosciences and Waisman Center, University of Wisconsin, Madison, Wisconsin, USA

Abstract

Fast axonal conduction depends on myelin, which is formed by Schwann cells in the PNS. We found that the transcription factor Yin Yang 1 (YY1) is crucial for peripheral myelination. Conditional ablation of *Yy1* in the Schwann cell lineage resulted in severe hypomyelination, which occurred independently of altered Schwann cell proliferation or apoptosis. In *Yy1* mutant mice, Schwann cells established a 1:1 relationship with axons but were unable to myelinate them. The Schwann cells expressed low levels of myelin proteins and of Egr2 (also called Krox20), which is an important regulator of peripheral myelination. *In vitro*, Schwann cells that lacked *Yy1* did not upregulate *Egr2* in response to neuregulin1 and did not express myelin protein zero. This phenotype was rescued by overexpression of *Egr2*. In addition, neuregulin-induced phosphorylation of YY1 was required for transcriptional activation of *Egr2*. Thus, YY1 emerges as an important activator of peripheral myelination that links neuregulin signaling with *Egr2* expression.

The ability of the nervous system to communicate with the periphery depends on faithful transmission of information to target tissues through peripheral nerves. The speed of propagation of action potentials in these nerves depends on myelin, which is formed by Schwann cells. Impaired differentiation of Schwann cells or damage to myelin results in debilitating peripheral neuropathies[1]. Given the clinical relevance of PNS myelination, it is not surprising that it has been the focus of several mechanistic studies. Investigation of the molecules at the axon-Schwann cell interface that trigger myelination led to the discovery of

Correspondence should be addressed to P.C. (patrizia.casaccia@mssm.edu).

Note: Supplementary information is available on the Nature Neuroscience website.

Author Contributions: Y.H. conducted the majority of the experiments and analyzed the data. J.Y.K. generated the YY1 point mutation plasmids and performed the immuno-precipitation and western blots. J.D. performed the ultrastructural analysis of the sciatic nerve. C.M.-V. and A.T. helped with the DRG co-culture experiments and conducted part of the *in vitro* myelination studies. J.S. performed the conservation analysis and contributed to the analysis of gene expression in the three mutants. P.C. supervised the project, analyzed the data, formatted the figures, uploaded microarray data and wrote the manuscript.

Competing Financial Interests: The authors declare no competing financial interests.

type III neuregulin1 (refs. 2–4). This axon-derived signal modulates almost every aspect of Schwann cell development and interacts with erbB2 and erbB3 receptors to initiate a signaling cascade that is essential for modulating the timing and abundance of myelin formation in peripheral nerves[2,4–7].

Many transcription factors also modulate Schwann cell differentiation, including Egr2, Pou3f1 (also known as Oct-6), Sox10, Brn1 and Brn2 (refs. 8–13). Among them, a key modulator of the transcriptional program of peripheral myelination is Egr2, a zinc finger transcription factor that is regulated by axonal contact and is induced as Schwann cells begin to myelinate. Analysis of *Egr2*-deficient mice and correlation of mutations in *EGR2* with human peripheral neuropathies have provided compelling evidence that Egr2 is important for myelination of peripheral nerves[10,14,15]. Gene expression studies have revealed that Egr2 acts as a positive regulator of the myelination process[16,17] although the molecular mechanisms that regulate its expression remain only partially understood. Egr2 is regulated by both soluble and membrane-bound neuregulins[4,16,18] and its concentration is partially modulated by calcium-dependent events[19].

Together these studies have indicated that peripheral myelination is the result of the interplay between extracellular signals and an intricate network of transcription factors, orchestrated by Egr2. However, many of the molecular connections between cell surface receptors and transcription factors that modulate myelination are unknown. We have identified the zinc finger protein YY1 as an important modulator of PNS myelination downstream of neuregulin1 (NRG1) signaling. The MEK-dependent cascade that was initiated by NRG1 treatment was responsible for activation of YY1 and increased expression of *Egr2*. In addition, Schwann cells that lacked YY1 owing to silencing or genetic ablation had low levels of Egr2 and showed impaired myelin gene expression, a phenotype that could be rescued by overexpression of Egr2.

Results

Severe hypomyelination in sciatic nerves lacking *Yy1*

We generated mutants with conditional ablation of *Yy1* in myelinating cells by crossing *Yy1 loxP*-flanked mice with the *Cnp-cre* line as described previously[20]. Although the mice were viable, the number of survivors decreased with age and dropped markedly after the third postnatal week (Supplementary Fig. 1a). In addition, surviving mice did not gain as much weight as their control siblings (Supplementary Fig. 1b). Heterozygous *Yy1* mice ($Yy1^{loxP/+}$; $Cnp\text{-}cre^{+/-}$) appeared normal and were used as littermate controls. We detected clinical signs of peripheral hypomyelination in the homozygous *Yy1* mutants ($Yy1^{loxP/loxP}$; $Cnp\text{-}cre^{+/-}$) during the second postnatal week; they were characterized by hindlimb weakness, flaccid tail paralysis and abnormal hindlimb posture reflexes (Fig. 1). The onset of clinical signs was consistent with the temporal profile of *Yy1* expression in the developing sciatic nerve. Yy1 was expressed at birth, but its transcript levels peaked at postnatal day (P)10 and its expression profile closely resembled that of *Egr2* during development[10,21] (Fig. 1b). Consistent with its role as transcription factor, we found YY1 in the nuclei of myelinated Schwann cells in wild-type mice (Fig. 1c) but not in the sciatic nerves of $Yy1^{loxP/loxP}$; $Cnp\text{-}cre^{+/-}$ mice (Fig. 1d).

Macroscopic examination of the sciatic nerves showed hypomyelination; the nerves were thick and opaque white in control mice and thin and translucent in *Yy1* mutants (Fig. 1e). At the molecular level, the sciatic nerves of $Yy1^{loxP/loxP}$; $Cnp\text{-}cre^{+/-}$ mice had lower levels of myelin gene transcripts than did those of control siblings. The differences in transcripts, including myelin protein zero (*Mpz*) and peripheral myelin protein 22 (*Pmp22*), between $Yy1^{loxP/loxP}$; $Cnp\text{-}cre^{+/-}$ and control siblings were not evident at P1, but became statistically

significant at P10 and persisted throughout development (Fig. 1f). Immunohistochemical analysis of MPZ confirmed the severe hypomyelination at P10 and P18 in the sciatic nerve of *Yy1*$^{loxP/loxP}$*; Cnp-cre*$^{+/-}$ mice and supported the idea that YY1 is important for myelination from P10 (Fig. 1g). At the ultrastructural level, the sciatic nerves of *Yy1*$^{loxP/loxP}$*; Cnp-cre*$^{+/-}$ mice at P18 had very few myelinated axons (14.3 ± 6.3%, total of 692 axons counted and three mice analyzed) compared with controls (54.7 ± 8.5%, 779 axons counted and three mice analyzed; Fig. 2a). The myelinated axons detected in *Yy1*$^{loxP/loxP}$*; Cnp-cre*$^{+/-}$ mice had thinner myelin sheaths, as indicated by the greater *g* ratio (ratio of axon diameter to the myelinated fiber diameter) in *Yy1* mutants (0.853 ± 0.076) compared with controls (0.691 ± 0.088; Fig. 2b).

In *Yy1*$^{loxP/loxP}$*; Cnp-cre*$^{+/-}$ mice we detected Schwann cells in a 1:1 relationship with large caliber axons (>1 μm), but the percentage of unmyelinated large caliber axons was much greater than in controls (Fig. 2c). Because peripheral nerve myelination proceeds in sequential stages that include the association of Schwann cells with clustered axons, followed by radial sorting and 1:1 segregation with the axon[1], our data suggested that the sorting process was not affected in *Yy1*$^{loxP/loxP}$*; Cnp-cre*$^{+/-}$ mice and that only the late stages of myelination were impaired. In addition, high levels of Pou3f1 (a marker of pro-myelinating cells) persisted in *Yy1*$^{loxP/loxP}$*; Cnp-cre*$^{+/-}$ mice (Fig. 2d,e). Consistent with impaired developmental myelination, we rarely saw adjacent myelin segments in *Yy1*$^{loxP/loxP}$*; Cnp-cre*$^{+/-}$ sciatic nerves and we noted the prevalence of heminodes (half of a node characterized by the presence of an unpaired paranode; Fig. 2f). The ultrastructural appearance of heminodes in *Yy1* mutants at P18 was consistent with the immunohistochemical detection of unpaired clusters of contactin-associated paranode protein (Caspr) labeling (Fig. 2f). This further confirmed the hypomyelinating phenotype.

We also observed defective myelination in the absence of *Yy1 in vitro*, in dorsal root ganglia (DRG) explants (Supplementary Fig. 2a,b), which contained neurons and Schwann cell precursors[22]. In explants from control siblings DRG axons were effectively myelinated (18.1 ± 4.7 myelin segments per field; Fig. 3a), whereas myelination was rare in explants from *Yy1*$^{loxP/loxP}$*; Cnp-cre*$^{+/-}$ mice (2.1 ± 1.1 myelin segments per field; Fig. 3b). The lack of myelinated segments correlated with low levels of myelin gene transcripts (Fig. 3c) and severely decreased myelin protein levels, as detected by protein blot (Fig. 3d). To further characterize the effect of YY1 on Schwann cell myelination, we repeated the experiment with DRG explants isolated from *Yy1*$^{loxP/loxP}$;*Plp-CreER*^{T} embryos[23] at embryonic day (E)13.5, in which *Yy1* was deleted in myelinating cells in a tamoxifen-inducible manner[23] (Fig. 3e,f). We determined the efficiency of recombination in myelinating Schwann cells by treating cultures with 10 nM, 100 nM and 1 μM 4-hydroxy-tamoxifen (4OH-TM) for 48 h and assaying the nuclear localization of Cre and the expression of YY1 using immunocytochemistry (Supplementary Fig. 2c). As expected, 4OH-TM induced nuclear translocation of Cre in a dose-dependent fashion only in Schwann cells, but not in fibroblasts and neurons, that continued to express YY1 (Supplementary Fig. 2c). The analysis of myelin segments in explants treated with 1 μM 4OH-TM (Fig. 3f) revealed only 2.2 ± 0.6 myelin segments per field compared to 20.5 ± 4.9 segments in mock-treated explants and 15.3 ± 2.9 segments in *Yy1*$^{loxP/loxP}$ explants treated with 4OH-TM (Fig. 3e). To confirm that defective myelination in the *Yy1*$^{loxP/loxP}$*; Cnp-cre*$^{+/-}$ explants depended on the Schwann cells and not on the DRG neurons, we generated co-cultures of wild-type rat Schwann cells with DRG neurons from *Yy1*$^{loxP/loxP}$*; Cnp-cre*$^{+/-}$ or control embryos (Fig. 3g). Both cultures showed similar numbers of myelin segments, which supports the idea that the defect in the *Yy1*$^{loxP/loxP}$*; Cnp-cre*$^{+/-}$ mice depended on Schwann cell function.

YY1 is an important upstream regulator of *Egr2*

We reasoned that the mechanism of action of YY1 in Schwann cells might involve *Egr2* because the two transcripts shared a similar expression profile in the developing sciatic nerve and because of the marked similarities between the phenotype of the *Yy1*$^{loxP/loxP}$; *Cnp-cre*$^{+/-}$ mice and those of *Egr2*$^{Lo/Lo}$ mutants[10,14] and Egr2-binding protein *Nab1* (*NGFI-A binding protein 1*)$^{-/-}$; *Nab2* (*NGFI-A binding protein 2*)$^{-/-}$ double mutants[17]. In all three mutant mice, similar clinical signs developed during the second postnatal week and included tremor and weakness of the hind limbs. The macroscopic appearance of the sciatic nerves was identical (thin and translucent) and the Schwann cells in the three mutants showed successful completion of radial sorting and defective myelination[10,14,17]. Because *Egr2*$^{Lo/Lo}$ (refs. 10,14,24) and *Nab1*$^{-/-}$; *Nab2*$^{-/-}$ double mutants[17] showed increased proliferation and apoptosis compared to control mice, we investigated whether similar features occurred in the *Yy1*$^{loxP/loxP}$; *Cnp-cre*$^{+/-}$ mice. We used BrdU incorporation to measure S-phase entry and performed immunohistochemical analysis of the sciatic nerve of *Yy1* mutant and control mice at P1, P10 and P18 (Fig. 4a,b). Although we detected no difference at the early developmental time points, similar to the *Egr2*$^{Lo/Lo}$ mice[14], we found a higher percentage of BrdU^{+} cells in the sciatic nerves of *Yy1*$^{loxP/loxP}$; *Cnp-cre*$^{+/-}$ mice than in those of controls at P10 and P18 (Fig. 4b). The detection of a proliferative phenotype at p10, but not at p1, in *Yy1*$^{loxP/loxP}$; *Cnp-cre*$^{+/-}$ mice was consistent with the developmental pattern of *Yy1* expression in the sciatic nerve and correlated with the downregulation of the cell cycle inhibitor Cdkna1 (also called p21), which is an important regulator of the G1-S phase transition (Fig. 4c). We detected similar results in DRG co-cultures from *Yy1*$^{loxP/loxP}$; *Cnp-cre*$^{+/-}$ mice and controls (Supplementary Fig. 3). We next examined apoptosis in the sciatic nerves. Although we found no difference at P2 or P10, we detected a transient and modest increase in TUNEL^{+} cells at P18 in *Yy1*$^{loxP/loxP}$; *Cnp-cre*$^{+/-}$ mice compared with controls (Fig. 4d). This was associated with increased transcripts of genes involved in apoptosis, such as *Jun* and *Tgfb1* (refs. 25,26; Fig. 4e). Together, these data suggested that there might be a genetic interaction between YY1 and Egr2.

To investigate this possibility, we compared gene profiling of the sciatic nerves from control and *Yy1*$^{loxP/loxP}$; *Cnp-cre*$^{+/-}$ mice at P21 and identified 1,575 upregulated genes and 1,151 downregulated genes. We then compared this set of 2,725 genes with published gene profiling datasets from *Egr2*$^{Lo/Lo}$ and *Nab1*$^{-/-}$; *Nab2*$^{-/-}$ mice[17]. Among the genes whose expression changed in *Yy1* mutants, 36.67% were also changed in *Egr2*$^{Lo/Lo}$ mice and 24.60% were also altered in *Nab1*$^{-/-}$; *Nab2*$^{-/-}$ mice. Of the regulated genes, 351 overlapped in all three mutants (Fig. 5a). The shared subsets of genes that had decreased expression included the myelin genes *Pmp22, Mpz* and *Mbp*, and those encoding lipid metabolism enzymes such as stearoyl-coenzyme A desaturase 2 (*Scd2*), fatty acid desaturase 2 (*Fads2*), 24-dehydrocholesterol reductase (*Dhcr24*) and HMG coenzyme A reductase (*Hmgcr*; Fig. 5b), and this is consistent with the hypomyelinating phenotype and with the involvement of these genes in several human neuropathies. Additional transcripts that were significantly decreased in all three mutants included several growth factors such as fibroblast growth factor 1 (*Fgf1*), *Fgf4* and bone morphogenetic protein 7 (*Bmp7*), and receptors such as Frizzled-related protein 3 (*Frzb*) and G protein-coupled receptor family C group 5 (*Gprc5b*). The transcripts that were upregulated during the third postnatal week in all three mutants included the transcription factors *Sox4, Sox5, Egr1, Pou3f1, Btg1, Id2* and *Id4* (refs. 27,28; Fig. 5b) and also genes related to the cell cycle such as cyclin B1 (*Ccnb1*), cyclin D1 (*Ccnd1*), cell division cycle associated 3 (*Cdca3*) and pituitary tumor-transforming 1 (*Pttg1*).

The similarity between the gene expression signatures in the sciatic nerves of *Egr2*$^{Lo/Lo}$ mice and *Yy1*$^{loxP/loxP}$; *Cnp-cre*$^{+/-}$ mice was consistent with a possible interaction between YY1 and the Egr2-Nab regulatory network. As the levels of *Yy1* transcript changed only

slightly in *Egr2*$^{Lo/Lo}$ mice (1.2-fold) and in *Nab1*$^{-/-}$; *Nab2*$^{-/-}$ mice (0.95-fold)[14,17], it was unlikely that *Yy1* was downstream of the Egr2–Nab complex. An alternative possibility was that *Yy1* was upstream of *Egr2*. Indeed, levels of *Egr2* transcripts in the sciatic nerve of *Yy1*$^{loxP/loxP}$; *Cnp-cre*$^{+/-}$ mice were significantly lower than control values at P10 and reached 38 ± 8% of control levels at P21 (Fig. 5c). Levels of *Nab1* transcript were less affected in *Yy1*$^{loxP/loxP}$; *Cnp-cre*$^{+/-}$ mice (62 ± 6.3% of the level of the controls, $n = 3$) and *Nab2* transcripts were increased (70% more than controls), which suggests that the effect of Yy1 on myelination was unlikely to be mediated by the modulation of Nab1 and Nab2 levels (Fig. 5d). The decrease in *Egr2* transcripts in *Yy1*$^{loxP/loxP}$; *Cnp-cre*$^{+/-}$ mice was consistent with the detection of decreased levels of Egr2 protein by immunohistochemistry (Fig. 5e) and protein blot (Fig. 5f). To prove that Egr2 was downstream of YY1, we overexpressed Egr2 in *Yy1*$^{loxP/loxP}$; *Cnp-cre*$^{+/-}$ Schwann cells; this overexpression rescued the expression of MPZ (Fig. 5f). Together these data provide strong evidence that YY1 is an upstream regulator of *Egr2*.

To investigate whether the hypomyelinating phenotype of *Yy1* mutants resulted from changes in the expression of genes that negatively affect postnatal peripheral myelination, we searched the microarray database for enrichment in genes in the Notch signaling pathway[29]. We also searched for genes related to the neuregulin-calcineurin-NFATcy pathway, which modulates Schwann cell differentiation[19]. Pathway analysis conducted with the DAVID Gene Functional Classification Tool did not reveal any enrichment of genes associated with these two signaling pathways (data not shown). To test further whether the decrease in *Egr2* transcripts in *Yy1*$^{loxP/loxP}$; *Cnp-cre*$^{+/-}$ mice resulted from altered Notch signaling, we performed protein blot analysis and quantitative real-time PCR. The decreased levels of the intracellular domain of Notch (NICD) detected in *Yy1*$^{loxP/loxP}$; *Cnp-cre*$^{+/-}$ mice (Fig. 5g), together with the similar levels of Notch1 and its ligand Jagged1 throughout development (Fig. 5h), ruled out the involvement of this pathway in the hypomyelinating phenotype of the mutants. Similarly, the pattern of expression of calcineurin B (*Cnb1*, also known as *Ppp3r1*; Fig. 5h) and the lack of similarities between the phenotypes of *Yy1*$^{loxP/loxP}$; *Cnp-cre*$^{+/-}$ and *Ppp3r1* mutant mice suggested that YY1 acts as upstream regulator of Egr2, independent of calcineurin B or Notch signaling.

NRG1-dependent YY1 phosphorylation regulates *Egr2*

The expression of *Egr2* expression is crucial for peripheral nerve myelination and is regulated by axonal contact and soluble neuregulin[4,17]. Treatment of cultured Schwann cells[17,18] with soluble NRG1 for 1 h was sufficient to induce upregulation of *Egr2* transcripts (Fig. 6a). To determine whether YY1 was part of the signaling pathway that was responsible for the upregulation of *Egr2* in response to NRG1, we silenced its expression using short hairpin RNA (shRNA) plasmids transfected into primary Schwann cells (Fig. 6b) and measured the transcript levels (Fig. 6c). *Yy1* silencing significantly decreased the NRG1-mediated expression of *Egr2* transcripts (Fig. 6c) whereas the levels of *Nab1*, *Nab2* and *Pou3f1* transcripts remained unchanged (Fig. 6d).

The role of YY1 in regulating the NRG-induced expression of *Egr2* was consistent with the presence of multiple YY1 binding sites in the promoter and conserved regulatory region (MSE, myelinating Schwann cell element) of *Egr2* (Supplementary Fig. 4). To test the effect of YY1 on the activity of the *Egr2* promoter and MSE, we performed a series of cotransfection experiments with YY1 constructs and luciferase reporter genes, driven either by the mouse *Egr2* promoter or by the MSE region upstream of a minimal promoter[19]. We treated cotransfected Schwann cells with NRG1 and measured reporter activity. Consistent with the role of YY1 as an NRG1-dependent downstream activator of *Egr2*, we detected increased reporter activity in cotransfected cells only after treatment with NRG1 (Fig. 6e).

To determine whether YY1 directly modulated the activity of the *Egr2* promoter and MSE in living cells, we performed chromatin immunoprecipitation (ChIP). Chromatin was cross-linked from Schwann cells before or after exposure of Schwann cells to NRG1 for 1 or 12 h. We then tested the recruitment of YY1 to precise chromatin loci using immunoprecipitation with antibodies to YY1 followed by quantitative ChIP with primers specific for the *Egr2* locus (Fig. 7a). YY1 was recruited to the promoter and MSE region of *Egr2* only after treatment with NRG1 for 1 h (Fig. 7b) and was consistent with the kinetics of *Egr2* transcription in response to NRG1 (Fig. 6a).

We next investigated how NRG1 treatment promoted binding of YY1 to the *Egr2* locus. Because neither the levels nor the subcellular localization of YY1 changed upon NRG1 treatment (Fig. 7c), we investigated whether its activity was modulated by post-translational modifications induced by NRG1. Analysis of the amino acid sequence of YY1 revealed several potential phosphorylation sites that were highly conserved among species (Fig. 7d). These sites were consistent with the results of proteomic studies in which YY1 was found to be phosphorylated on S118, S184 and S247 in Hela cells[30,31]. Analysis of the sequences that surrounded these serine residues, using the Group-based Prediction System[32], indicated that these residues were potential MEK phosphorylation sites. Because activation of the MEK-MAPK cascade has been identified as part of NRG1 signaling, we defined the time course of serine phosphorylation of YY1 in Schwann cells exposed to NRG1. Protein extracts from Schwann cells treated with NRG1 for 20 min or 1 h were immunoprecipitated with YY1 antibodies and processed for protein blot analysis using anti-phospho-serine antibodies. We detected an immunoreactive band in the 1-h treatment sample, which indicated YY1 phosphorylation (Fig. 7e).

To identify the kinase that phosphorylated YY1 in response to NRG1, we tested the functional consequences of pharmacologically blocking the three main pathways downstream of NRG1 (refs. 3,19). We used inhibitors of Akt activity (LY294002), MEK kinase (U0126 and PD98059) and the phospholipase C (PLC)γ-calcineurin pathway (cyclosporin A (CsA)). Of these compounds, the MEK inhibitors most severely impaired the NRG1-mediated increase in *Egr2* expression (Fig. 8a) and blocked YY1 phosphorylation (data not shown). Using ChIP, we also showed that the recruitment of YY1 to the MSE regions of the *Egr2* locus in response to NRG1 treatment was impaired by treatment with U0126 but not with CsA (Fig. 8b).

To determine the functional role of NRG1-induced phosphorylation of YY1, we generated multiple Ser→Ala mutantions at position 118, 184 and 247 of YY1 and tested the consequences for the transcriptional activity of YY1 using a YY1 TransLucent Reporter[20]. Mutation of one, two or three serine residues impaired the ability of YY1 to activate a luciferase reporter driven by a *cis*-acting enhancer element containing multiple YY1 binding sites upstream of a minimal promoter after NRG treatment (Fig. 8c). Although single Ser→Ala substitutions only moderately affected the ability of YY1 to transactivate luciferase reporters driven by the *Egr2* regulatory elements (Fig. 8d), the mutant construct with three amino acid substitutions produced the most significant impairment (Fig. 8d). Therefore, phosphorylation of YY1 is a key signal downstream of NRG1 that is required for the upregulation of *Egr2*.

Our results identify YY1 as a crucial regulator of peripheral nerve myelination that functions as an activator upon NRG1-dependent phosphorylation of key serine residues.

Discussion

YY1 is a key regulator of postnatal myelination in the PNS

The notable peripheral nerve hypomyelination that we detected in mice with conditional ablation of *Yy1* provides the first *in vivo* genetic evidence that YY1 has a crucial role in peripheral nerve myelination. The expression of YY1 in the developing sciatic nerve paralleled that of the key transcriptional regulator Egr2, which has been extensively characterized for its role in promoting the attainment of a myelinating phenotype[10,21]. The temporal expression profile of YY1 suggested that it might be involved in the late postnatal development of peripheral nerves. Consistent with this prediction, at birth the sciatic nerves of $Yy1^{loxP/loxP}$; $Cnp\text{-}cre^{+/-}$ mice and control mice were similar in appearance. The proliferation rates, numbers and gene expression profiles of Schwann cells were also similar between wild-type and $Yy1^{loxP/loxP}$; $Cnp\text{-}cre^{+/-}$ mice during the first neonatal days. Early Schwann cell development was therefore unperturbed in the $Yy1^{loxP/loxP}$; $Cnp\text{-}cre^{+/-}$ mice and the detection of a correct 1:1 relationship with the axons confirmed that Schwann cells underwent radial sorting and axonal segregation. We observed severe hypomyelination during the second postnatal week, characterized by decreased levels of myelin proteins and of Egr2.

Notably, the presence of hypomyelination after normal segregation, increased proliferation and compensatory apoptosis at P10 resembled the phenotype of *Egr2* mutants[10,14]. A comparison between the gene expression profiles of *Yy1* deficient mice and *Egr2* hypomorphs revealed marked similarities in the patterns of gene expression in the peripheral nerves of these mutants[14]. The ability of Egr2 to rescue the ability of cultured *Yy1* mutant Schwann cells to express myelin proteins suggested that *Egr2* is downstream of *Yy1*. This conclusion was supported by evidence that overexpression of *Yy1* activated the expression of luciferase reporter genes driven by the *Egr2* promoter and regulatory elements and that YY1 is physically bound to these elements in the chromatin of cultured Schwann cells exposed to NRG1.

YY1 activity is regulated by NRG1-dependent phosphorylation

Myelination of the PNS depends on the interplay between extracellular signals and a complex transcriptional network that modulates Schwann cell maturation. Previous work has shown that NRG1 type III is the axonal signal that binds to its receptors erbB2 and erbB3 and regulates the timing and amount of myelination as well as myelin sheath thickness[2,4]. Besides its role in myelination, NRG1 also regulates multiple stages of Schwann cell development, including the early commitment of neural crest cells and precursor migration[1,6], and several groups have attempted to decipher the signaling events downstream of the activation of erbB2 and erbB3 receptors.

A crucial event in myelination is the upregulation of Egr2. The levels of Egr2 are increased during the transition to myelinating Schwann cells and this increase has been attributed to axonal contact as well as to membrane-bound or soluble neuregulins[4,17]. Despite the evidence that Egr2 is crucial for peripheral nerve myelination, there is limited information on the NRG1-dependent pathways that regulate *Egr2* expression. Three signaling pathways have been shown to be activated by erbB2–erbB3 receptor complexes in response to ligand binding: phosphatidylinositol-3-OH kinase (PI(3)K), PLCγ and MEK[19,33–35]. Although many reports have focused on the activation of the PI(3)K pathway, a recent study has implicated the PLCγ pathway, in cooperation with Sox10, in activating the transcription of *Egr2* and *Mpz*[19]. It has been proposed that Ca^{2+} influx, mediated by the PLCγ pathway and followed by activation of calcineurin and dephosphorylation of NFATc4, activates *Egr2* and *Mpz*. However the analysis of sciatic nerves from mice with mutations in *Ppp3r1* showed

substantial levels of *Egr2* transcripts and therefore suggested that there are alternative pathways of activation of *Egr2* in the absence of calcineurin B[19]. We have provided several lines of evidence that YY1 is a key regulator of *Egr2*. First, we have defined the *in vivo* kinetics of binding of YY1 to the chromatin in the promoter and MSE regulatory region of *Egr2* upon exposure of Schwann cells to NRG1. Second, we have shown that silencing of *Yy1* prevents the NRG1-dependent increase in *Egr2*, without affecting the levels of *Pou3f1*, *Nab1* or *Nab2*. Third, we have shown that the NRG1-dependent serine phosphorylation of YY1 is crucial for the recruitment of YY1 to the *Egr2* locus and that it depends on the activation of the MEK cascade (Supplementary Fig. 6). Previous studies had identified the downstream MAPKs as mediators of the proliferative and migratory effects of NRG1 in Schwann cell precursors[35,36]. Our data are not inconsistent with this possibility, because we focused our analysis at the postnatal stage of development, when YY1 is increased, rather than at earlier embryonic stages. Downstream of MEK kinase, at least two pathways with opposing effects have been identified. The activation of the Ras-MAPK pathway, for instance, has been associated with lack of differentiation[34,37,38], whereas activation of p38 kinase has been associated with myelination[37,39]. However, these effects were dependent on the concentrations of soluble NRG and the strength of MAPK activation. Together these data suggest that in Schwann cells, as in other experimental systems, exposure to signaling molecules (NRG1) determined an outcome that depended on the strength of the signal, the enzymes that were activated (Akt, PLCγ, MEK), the levels and kinetics of activation of each enzyme and the specificity of the cellular substrates, which may differ at distinct developmental stages. Future studies might be needed to determine the molecular identity and functional significance of NRG-dependent activation at distinct stages in Schwann cell development and in response to exposure to axon-bound or soluble ligands.

The role of YY1 is unique and cell-type specific

In oligodendrocytes, the myelin-forming cells of the CNS, YY1 forms repressive complexes with HDAC1 and HDAC2 that downregulate transcriptional inhibitors of myelin gene expression, such as Tcf7l2 and Id4, and favor progression to a myelinating phenotype[20]. In other words, YY1 modulates oligodendrocyte differentiation by promoting a de-repression mechanism (inhibiting the inhibitors). Considering that both oligodendrocytes and Schwann cells can produce myelin and that their differentiation is similarly impaired in the absence of *Yy1*, the simplest explanation would suggest that YY1 has a similar role in myelin-forming cells of the PNS and CNS. However, we have shown that the role of YY1 in the PNS is quite different from its role in the CNS and that it acts as transcriptional activator of *Egr2*, a key regulator of Schwann cell myelination. The ability of YY1 to activate the expression of *Egr2* is not constitutive, but rather is modulated by phosphorylation events that can be induced by exposure of Schwann cells to NRG1. Therefore, even though the peripheral and central phenotypes of *Yy1* mutant mice are similar (hypomyelination), the YY1-dependent mechanisms in the CNS and PNS are distinct and cell specific. In oligodendrocytes, YY1 is part of repressive complexes that contain histone deacetylases and the repression of transcriptional inhibitors depends on its acetylation state[40]. By contrast, in Schwann cells YY1 functions as activator of gene expression whose activity depends on the phosphorylation state of specific serine residues, consistent with early studies on the signals that modulate the yin and yang functions of this zinc-finger protein[41].

The essential function of YY1 in Schwann cell myelination, as revealed by the phenotype of *Yy1* conditional knockout mice, does not exclude the possibility that YY1participates in earlier stages of Schwann cell development. *Yy1* deletion studies in *Xenopus* have identified several target genes that are involved in neural crest development, such as *slug, snail* and *Otx2* (refs. 42,43). It will be interesting to determine whether YY1 has distinct functions at different stages of Schwann cell lineage development and to identify the post-translational

modifications of this transcription factor that might integrate the cross-talk among distinct signaling pathways.

Methods

Methods and any associated references are available in the online version of the paper at http://www.nature.com/natureneuroscience/.

Supplementary Material

Refer to Web version on PubMed Central for supplementary material.

Acknowledgments

We thank Y. Shi, K.A. Nave and B. Popko for mouse lines; G. Crabtree, D. Meijer and M. Grumet for plasmids and antibodies; H. Kim and P. Maurel for advice on Schwann cell and myelination cultures; C. Krier for assistance with microarrays; J. Salzer, K. Jessen, P. Brophy and C. Taveggia for discussions; and N. Kuo, J. Li and R. Srinivasan for technical assistance. This work was supported by grant numbers 5R01NS042925-08, R01NS052738-04 and NS04295-08S ARRA supplement and NMSS RG-4134 to P.C. and in part by the NJ Commission on Spinal Cord Research (08B-010-SCR3 to Y.H.). Electron microscopy was performed at the VCU Department of Anatomy and Neurobiology Microscopy Facility and supported, in part, by funding from a US National Institutes of Health Natinal Institute of Neurological Disorders and Stroke Center core grant (5P30NS047463-02).

References

1. Jessen KR, Mirsky R. The origin and development of glial cells in peripheral nerves. Nat Rev Neurosci. 2005; 6:671–682. [PubMed: 16136171]
2. Michailov GV, et al. Axonal neuregulin-1 regulates myelin sheath thickness. Science. 2004; 304:700–703. [PubMed: 15044753]
3. Nave KA, Salzer JL. Axonal regulation of myelination by neuregulin 1. Curr Opin Neurobiol. 2006; 16:492–500. [PubMed: 16962312]
4. Taveggia C, et al. Neuregulin-1 type III determines the ensheathment fate of axons. Neuron. 2005; 47:681–694. [PubMed: 16129398]
5. Chan R, Hardy WR, Dankort D, Laing MA, Muller WJ. Modulation of Erbb2 signaling during development: a threshold level of Erbb2 signaling is required for development. Development. 2004; 131:5551–5560. [PubMed: 15496447]
6. Garratt AN, Voiculescu O, Topilko P, Charnay P, Birchmeier C. A dual role of erbB2 in myelination and in expansion of the Schwann cell precursor pool. J Cell Biol. 2000; 148:1035–1046. [PubMed: 10704452]
7. Chen S, et al. Neuregulin 1-erbB signaling is necessary for normal myelination and sensory function. J Neurosci. 2006; 26:3079–3086. [PubMed: 16554459]
8. Jaegle M, et al. The POU proteins Brn-2 and Oct-6 share important functions in Schwann cell development. Genes Dev. 2003; 17:1380–1391. [PubMed: 12782656]
9. Jaegle M, et al. The POU factor Oct-6 and Schwann cell differentiation. Science. 1996; 273:507–510. [PubMed: 8662541]
10. Topilko P, et al. Krox-20 controls myelination in the peripheral nervous system. Nature. 1994; 371:796–799. [PubMed: 7935840]
11. Britsch S, et al. The transcription factor Sox10 is a key regulator of peripheral glial development. Genes Dev. 2001; 15:66–78. [PubMed: 11156606]
12. Friedrich RP, Schlierf B, Tamm ER, Bosl MR, Wegner M. The class III POU domain protein Brn-1 can fully replace the related Oct-6 during schwann cell development and myelination. Mol Cell Biol. 2005; 25:1821–1829. [PubMed: 15713637]
13. Ryu EJ, et al. Misexpression of Pou3f1 results in peripheral nerve hypomyelination and axonal loss. J Neurosci. 2007; 27:11552–11559. [PubMed: 17959798]

14. Le N, et al. Analysis of congenital hypomyelinating Egr2Lo/Lo nerves identifies Sox2 as an inhibitor of Schwann cell differentiation and myelination. Proc Natl Acad Sci USA. 2005; 102:2596–2601. [PubMed: 15695336]
15. Warner LE, et al. Mutations in the early growth response 2 (EGR2) gene are associated with hereditary myelinopathies. Nat Genet. 1998; 18:382–384. [PubMed: 9537424]
16. Svaren J, Meijer D. The molecular machinery of myelin gene transcription in Schwann cells. Glia. 2008; 56:1541–1551. [PubMed: 18803322]
17. Le N, et al. Nab proteins are essential for peripheral nervous system myelination. Nat Neurosci. 2005; 8:932–940. [PubMed: 16136673]
18. Murphy P, et al. The regulation of Krox-20 expression reveals important steps in the control of peripheral glial cell development. Development. 1996; 122:2847–2857. [PubMed: 8787758]
19. Kao SC, et al. Calcineurin/NFAT signaling is required for neuregulin-regulated Schwann cell differentiation. Science. 2009; 323:651–654. [PubMed: 19179536]
20. He Y, et al. The transcription factor Yin Yang 1 is essential for oligodendrocyte progenitor differentiation. Neuron. 2007; 55:217–230. [PubMed: 17640524]
21. Zorick TS, Syroid DE, Arroyo E, Scherer SS, Lemke G. The transcription factors SCIP and Krox-20 mark distinct stages and cell fates in Schwann cell differentiation. Mol Cell Neurosci. 1996; 8:129–145.
22. Päiväläinen S, et al. Myelination in mouse dorsal root ganglion/Schwann cell cocultures. Mol Cell Neurosci. 2008; 37:568–578. [PubMed: 18206387]
23. Doerflinger NH, Macklin WB, Popko B. Inducible site-specific recombination in myelinating cells. Genesis. 2003; 35:63–72. [PubMed: 12481300]
24. Zorick TS, Syroid DE, Brown A, Gridley T, Lemke G. Krox-20 controls SCIP expression, cell cycle exit and susceptibility to apoptosis in developing myelinating Schwann cells. Development. 1999; 126:1397–1406. [PubMed: 10068633]
25. Parkinson DB, et al. Krox-20 inhibits Jun-NH2-terminal kinase/c-Jun to control Schwann cell proliferation and death. J Cell Biol. 2004; 164:385–394. [PubMed: 14757751]
26. Parkinson DB, et al. Transforming growth factor beta (TGFbeta) mediates Schwann cell death *in vitro* and *in vivo*: examination of c-Jun activation, interactions with survival signals, and the relationship of TGFbeta-mediated death to Schwann cell differentiation. J Neurosci. 2001; 21:8572–8585. [PubMed: 11606645]
27. Mager GM, et al. Active gene repression by the Egr2. NAB complex during peripheral nerve myelination. J Biol Chem. 2008; 283:18187–18197. [PubMed: 18456662]
28. Stewart HJ, et al. Helix-loop-helix proteins in Schwann cells: a study of regulation and subcellular localization of Ids, REB and E12/47 during embryonic and postnatal development. J Neurosci Res. 1997; 50:684–701. [PubMed: 9418957]
29. Woodhoo A, et al. Notch controls embryonic Schwann cell differentiation, postnatal myelination and adult plasticity. Nat Neurosci. 2009; 12:839–847. [PubMed: 19525946]
30. Beausoleil SA, et al. Large-scale characterization of HeLa cell nuclear phosphoproteins. Proc Natl Acad Sci USA. 2004; 101:12130–12135. [PubMed: 15302935]
31. Nousiainen M, Sillje HH, Sauer G, Nigg EA, Korner R. Phosphoproteome analysis of the human mitotic spindle. Proc Natl Acad Sci USA. 2006; 103:5391–5396. [PubMed: 16565220]
32. Zhou FF, Xue Y, Chen GL, Yao X. GPS: a novel group-based phosphorylation predicting and scoring method. Biochem Biophys Res Commun. 2004; 325:1443–1448. [PubMed: 15555589]
33. Maurel P, Salzer JL. Axonal regulation of Schwann cell proliferation and survival and the initial events of myelination requires PI 3-kinase activity. J Neurosci. 2000; 20:4635–4645. [PubMed: 10844033]
34. Harrisingh MC, et al. The Ras/Raf/ERK signaling pathway drives Schwann cell dedifferentiation. EMBO J. 2004; 23:3061–3071. [PubMed: 15241478]
35. Meintanis S, Thomaidou D, Jessen KR, Mirsky R, Matsas R. The neuron-glia signal beta-neuregulin promotes Schwann cell motility via the MAPK pathway. Glia. 2001; 34:39–51. [PubMed: 11284018]

36. Kim HA, DeClue JE, Ratner N. cAMP-dependent protein kinase A is required for Schwann cell growth: interactions between the cAMP and neuregulin/tyrosine kinase pathways. J Neurosci Res. 1997; 49:236–247. [PubMed: 9272646]

37. Fragoso G, et al. Inhibition of p38 mitogen-activated protein kinase interferes with cell shape changes and gene expression associated with Schwann cell myelination. Exp Neurol. 2003; 183:34–46. [PubMed: 12957486]

38. Zanazzi G, et al. Glial growth factor/neuregulin inhibits Schwann cell myelination and induces demyelination. J Cell Biol. 2001; 152:1289–1299. [PubMed: 11257128]

39. Haines JD, Fragoso G, Hossain S, Mushynski WE, Almazan G. p38 Mitogen-activated protein kinase regulates myelination. J Mol Neurosci. 2008; 35:23–33. [PubMed: 17994198]

40. He Y, Sandoval J, Casaccia-Bonnefil P. Events at the transition between cell cycle exit and oligodendrocyte progenitor differentiation: the role of HDAC and YY1. Neuron Glia Biol. 2007; 3:221–231. [PubMed: 18634613]

41. Becker KG, Jedlicka P, Templeton NS, Liotta L, Ozato K. Characterization of hUCRBP (YY1, NF-E1, delta): a transcription factor that binds the regulatory regions of many viral and cellular genes. Gene. 1994; 150:259–266. [PubMed: 7821790]

42. Kwon HJ, Chung HM. Yin Yang 1, a vertebrate polycomb group gene, regulates antero-posterior neural patterning. Biochem Biophys Res Commun. 2003; 306:1008–1013. [PubMed: 12821143]

43. Morgan MJ, Woltering JM, In der Rieden PM, Durston AJ, Thiery JP. YY1 regulates the neural crest-associated slug gene in *Xenopus laevis*. J Biol Chem. 2004; 279:46826–46834. [PubMed: 15326190]

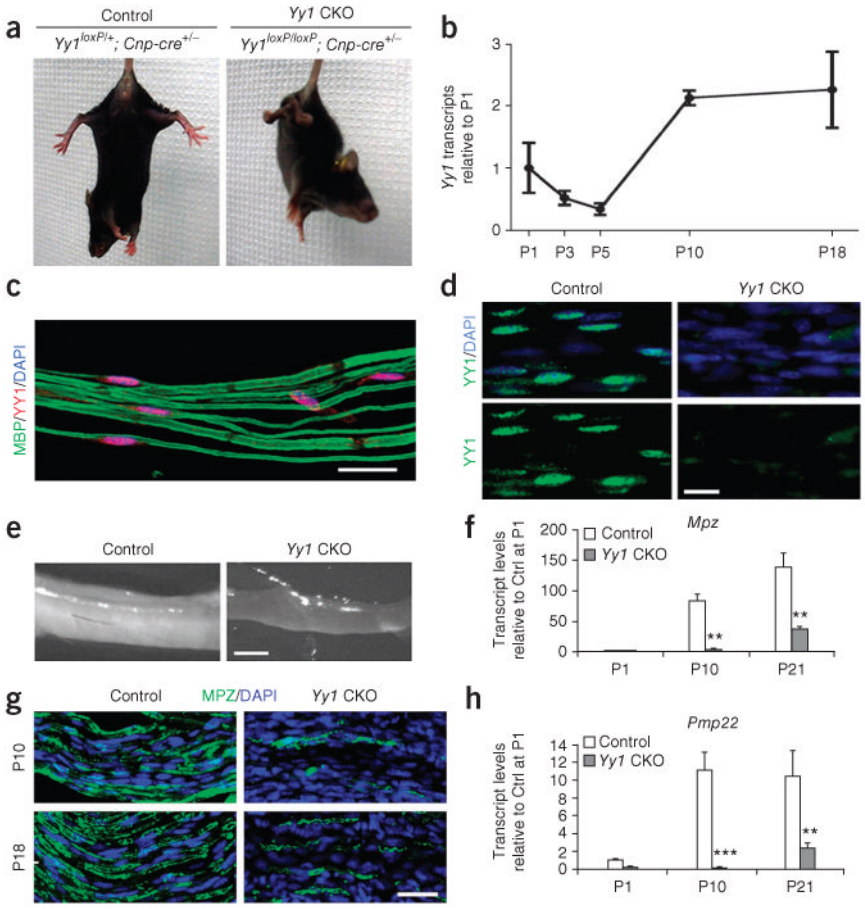

Figure 1.

Peripheral nerve hypomyelination in mice with conditional ablation of *Yy1*. (**a**) Normal hindlimb postural reflex in a P18 control mouse ($Yy1^{loxP/+}$; $Cnp\text{-}cre^{+/-}$), characterized by spreading of the limbs, and abnormal reflex in the mutant $Yy1^{loxP/loxP}$ $Cnp\text{-}cre^{+/-}$ mouse (CKO), characterized by crossing of the hind limbs. (**b**) Transcript levels of *Yy1* in mouse sciatic nerves during development measured using quantitative reverse transcription PCR (qRT-PCR) $n = 3$ at each time point). (**c**) Teased sciatic nerves from P21 wild-type mice stained for YY1 (red) and myelin basic protein (MBP; green) and processed for confocal analysis. Scale bar, 20 μm. (**d**) Immunohistochemistry for YY1 (green) in the sciatic nerve of controls but not in mutant ($Yy1^{loxP/loxP}$;$Cnp\text{-}cre^{+/-}$) mice at P18. Cell nuclei were counterstained with DAPI (blue). (**e**) Gross examination of sciatic nerves dissected from $Yy1^{loxP/loxP}$;$Cnp\text{-}cre^{+/-}$ and control mice at P18 show the white opaque appearance of control nerves and much thinner and more translucent appearance of mutant nerves. (**f**) qRT-PCR of RNA from sciatic nerves of $Yy1^{loxP/loxP}$;$Cnp\text{-}cre^{+/-}$ mice and control siblings at P1, P10 and P21. The bar graphs represent the transcript levels of *Mpz* and *Pmp22* relative to controls. Error bar, s.d.; $^{**}P < 0.01$, $^{***}P < 0.001$ ($n = 3$). (**g**) Longitudinal sections of the sciatic nerves from control and $Yy1^{loxP/loxP}$; $Cnp\text{-}cre^{+/-}$ mice at P10 and P18 were stained for MPZ (green) and nuclei were counterstained with DAPI (blue). Scale bars, 20 μm in **c, d, g** and 1 mm in **e**.

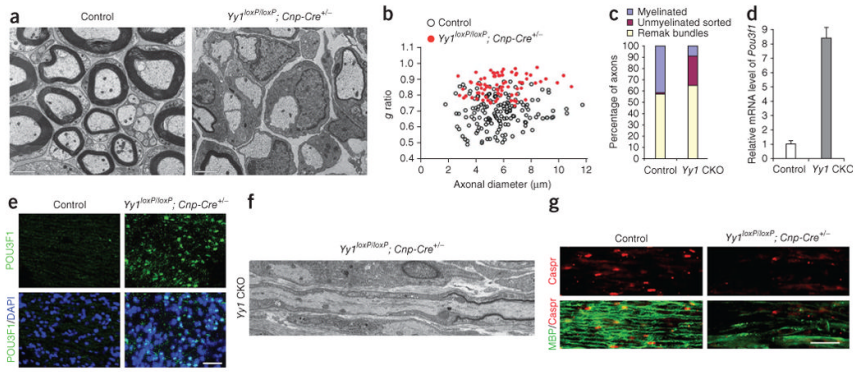

Figure 2.

Ablation of *Yy1* impairs the ability of Schwann cells to myelinate. (**a**) Electron micrographs of sciatic nerves of controls and *Yy1* mutants show severe hypomyelination in *Yy1*$^{loxP/loxP}$; *Cnp-cre*$^{+/-}$ mice at P18. The Schwann cells in the mutant mice established a 1:1 relationship with large-caliber axons but could not myelinate them. (**b**) Scatter plot indicating the *g* ratios of individual fibers as a function of axon diameter (*n* = 78 axons for *Yy1*$^{loxP/loxP}$; *Cnp-cre*$^{+/-}$ mice; *n* = 154 axons for controls). (**c**) Axons were classified into three categories: myelinated (blue bar), unmyelinated-sorted (red bar) and unmyelinated-Remak bundles (yellow bar) and quantified. (**d**) qRT-PCR revealed elevated *Pou3f1* transcripts in the sciatic nerves of *Yy1* mutant mice compared to controls. (**e**) Immunohistochemical validation of Pou3fl expression in longitudinal sections of the sciatic nerves from P18 *Yy1*$^{loxP/loxP}$; *Cnp-cre*$^{+/-}$ mice and control mice. (**f**) Electron micrographs of longitudinal sections of sciatic nerves in mutant mice showed heminodes, consisting of unpaired paranodal regions, whereas nodal regions were rarely detected. (**g**) Longitudinal sections of P18 sciatic nerves from control and *Yy1*$^{loxP/loxP}$; *Cnp-cre*$^{+/-}$ mice were stained for MBP (green) and for the paranodal protein Caspr (red). Note the uniform staining of myelinated MBP^{+} fibers and paired Caspr expression in control animals and the reduced level of MBP and disorganization of Caspr expression in mutant mice. Scale bars, 2 μm in **a**, 50 μm in **e** and 20 μm in **g**.

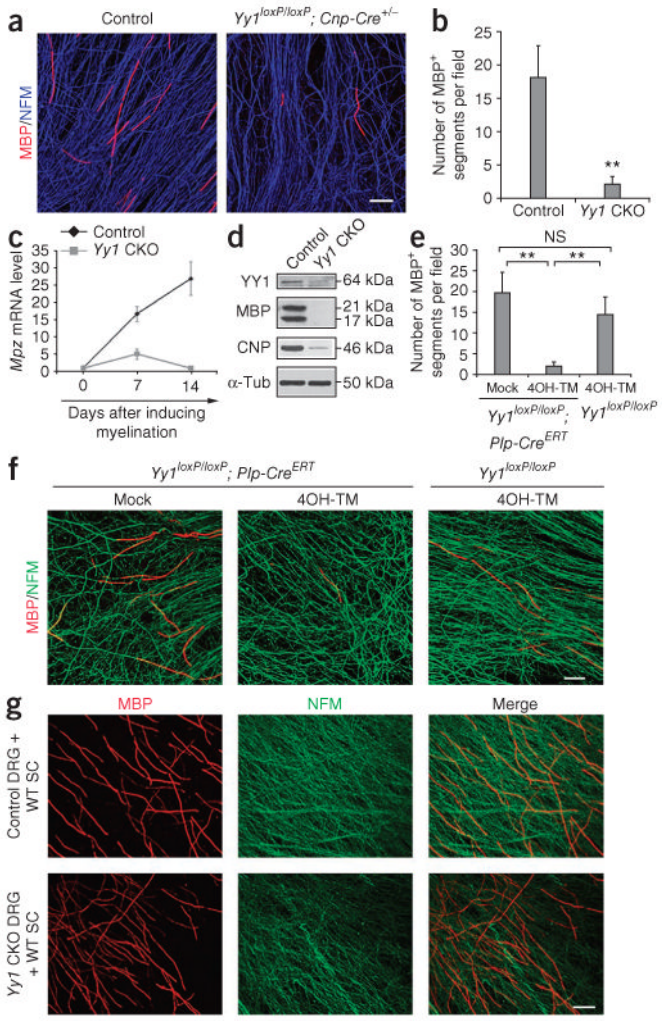

Figure 3.

Effect of *Yy1* ablation on the ability of Schwann cells to myelinate *in vitro*. (**a**) *In vitro* explant DRG cultures from E13.5 control and $Yy1^{loxP/loxP}$; $Cnp\text{-}cre^{+/-}$ embryos were immunostained for MBP (red) and neurofilament medium chain (NFM, blue). Note the few myelin segments in cultures from the $Yy1^{loxP/loxP}$; $Cnp\text{-}cre^{+/-}$ mice compared to controls. (**b**) Bar graph shows the number of myelin segments shown in a. (**c**) qRT-PCR of mRNA levels of *Mpz* in myelinating cultures established from $Yy1^{loxP/loxP}$; $Cnp\text{-}cre^{+/-}$ and control DRGs and examined at days 0, 7 and 14 after induction of myelination. (**d**) Protein blot analysis of MBP and CNPase in myelinating cocultures derived from $Yy1^{loxP/loxP}$; $Cnp\text{-}cre^{+/-}$ and control DRGs kept in culture for 21 d. Full-length blots are shown in Supplementary Figure 5. (**e,f**) Immunofluorescence of cocultures of DRG neurons and Schwann cells from E13.5 transgenic embryos ($Yy1^{loxP/loxP}$; *Plp-creERT*) treated with 1 μM Tamoxifen (4OH-TM) for 2 d and then cultured for additional 12 d to induce myelination. MBP (red) and neurofilament (NFM, green). (**g**) Immunofluorescence of $Yy1^{loxP/loxP}$; $Cnp\text{-}cre^{+/-}$ and control DRG neurons cultured with wild-type rat Schwann cells (WT SC) for 14 d and then stained for MBP (red) and NFM (green). Scale bars, 50 μm. Error bars, s.d.; $^{**}P < 0.01$.

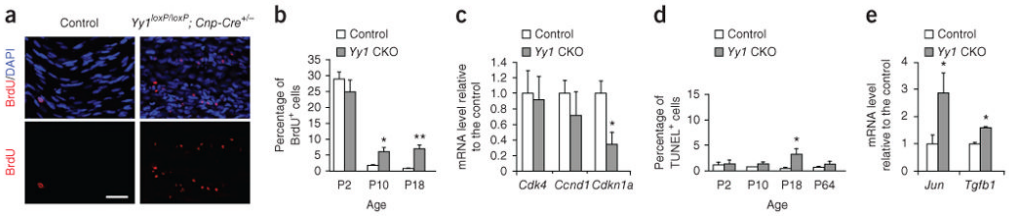

Figure 4.

Ablation of *Yy1* modulates Schwann cell S-phase entry during the second week of development. (**a**) Longitudinal sections of the sciatic nerves from P18 $Yy1^{loxP/loxP}$; $Cnp\text{-}cre^{+/-}$ and control mice stained with anti-BrdU (red) antibodies after 2 h pulse labeling of BrdU *in vivo*. Scale bar, 20 μm. (**b**) The fraction of $BrdU^+$ cells in the sciatic nerves at multiple developmental time points was quantified and referred to the percentage of $DAPI^+$ cells. (**c**) qRT-PCR of genes involved in proliferation (*Cdk4*, cyclin D1 (*Ccnd1*) and P21 (*Cdkn1a*)) in the sciatic nerves of mutant mice and control littermates at P10. (**d**) TUNEL assay of the sciatic nerves from mutant mice and control littermates at the indicated time points. The fraction of $TUNEL^+$ cells in the sciatic nerves was quantified and referred to the percentage of $DAPI^+$ cells. (**e**) qRT-PCR of genes involved in apoptosis (*Jun* and *Tgfb1*) in the sciatic nerves of mutant mice and control littermates at P21. Error bar, s.d.; $*P < 0.05$, $**P < 0.01$. $n = 3$ for each genotype at P2, P10, P18 and P21 and $n = 2$ at P64.

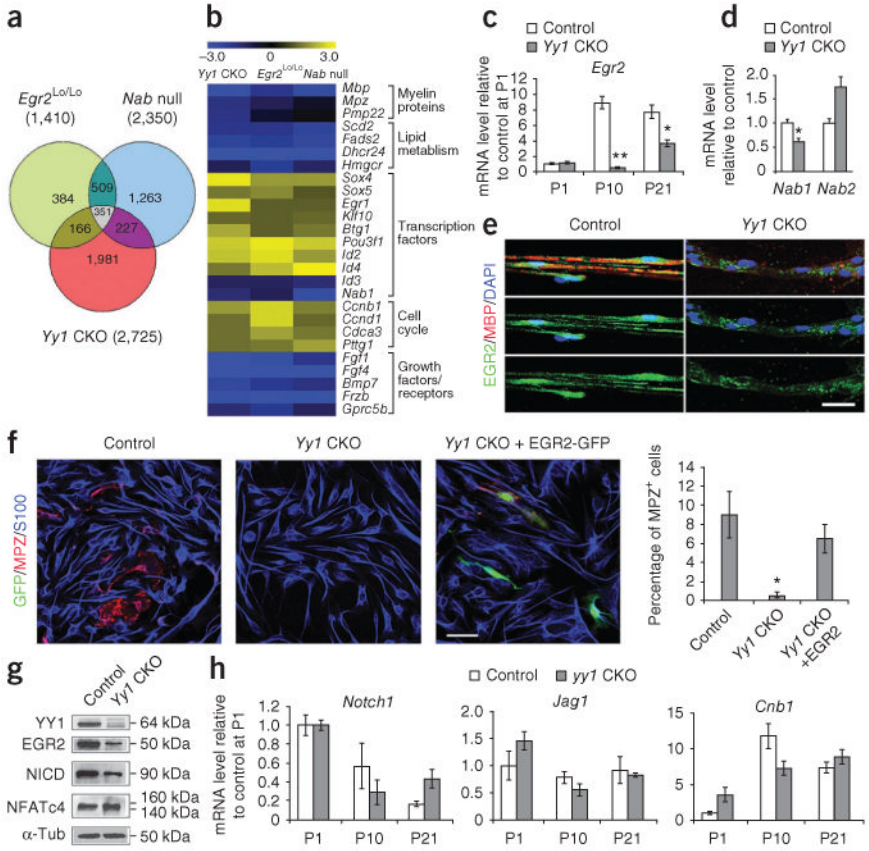

Figure 5.

YY1 regulates *Egr2* expression. (**a**) Intersection of genes altered in the sciatic nerves of *Yy1*$^{loxP/loxP}$*; Cnp-cre*$^{+/-}$ mice and of *Egr2*$^{Lo/Lo}$ and *Nab1*$^{-/-}$;*Nab2*$^{-/-}$ mice[17]. (**b**) Comparison of gene expression in *Yy1*$^{loxP/loxP}$*; Cnp-cre*$^{+/-}$, *Egr2*$^{Lo/Lo}$ and *Nab1*$^{-/-}$;*Nab2*$^{-/-}$ mice. Similar gene expression signatures in the sciatic nerves of the three mutants suggested that these molecules might share a common signaling pathway. The expression of *Nab1*, *Nab2* (**c**) and *Egr2* (**d**) was measured by qRT-PCR in the sciatic nerves at P21. (**e**) Immunohistochemistry showed decreased Egr2 (green) immunoreactivity in teased sciatic nerve fibers of *Yy1*$^{loxP/loxP}$*; Cnp-cre*$^{+/-}$ mice. (**f**) Purified mouse *Yy1*$^{loxP/loxP}$*; Cnp-cre*$^{+/-}$ Schwann cells cultured in myelination medium for 3 d showed normal S100 (blue) expression but low immunoreactivity for MPZ (red), and ectopic expression of *Egr2* in these cells rescued the phenotype as indicated by the detection of MPZ in GFP^{+} transfected cells. Bar graph shows quantification of the fraction of MPZ^{+} cells among S100^{+} cells from two experiments. (**g**) Protein blot of myelinating cocultures from *Yy1*$^{loxP/loxP}$*; Cnp-cre*$^{+/-}$ and control DRGs maintained for 21 d *in vitro* showed low Egr2, whereas the NICD was only mildly affected. Full-length protein blots are shown in Supplementary Figure 5. (**h**) qRT-PCR of *Notch1*, *Jag1* and *CnB1* in the sciatic nerves of *Yy1*$^{loxP/loxP}$*; Cnp-cre*$^{+/-}$ and control mice at distinct developmental time points. Error bar, s.d.; **P* < 0.05, ***P* < 0.01 (*n* = 3). Scale bars, 20 μm.

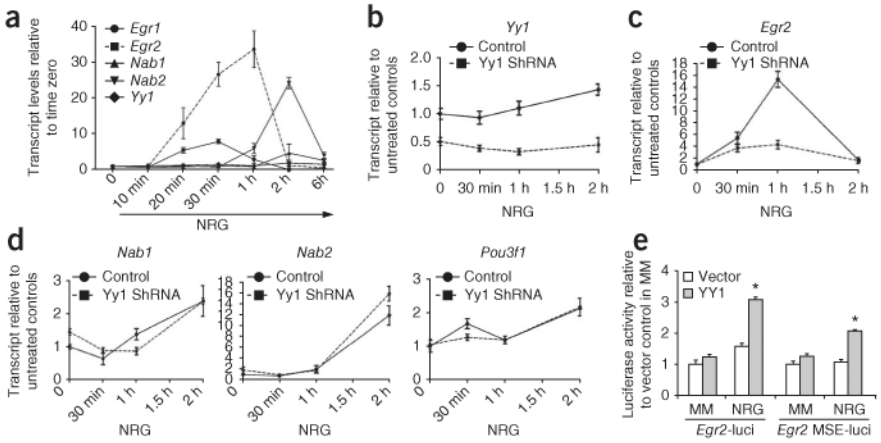

Figure 6.

YY1 regulates *Egr2* expression in response to NRG1. (**a**) Purified rat Schwann cells were cultured in minimal medium for 18 h and then exposed to NRG1. The transcript levels of *Egr1, Egr2, Nab1, Nab2* and *Yy1* at each time point were analyzed by qRT-PCR. *Egr2* transcripts increased at 20 min, peaked at 1 h and then gradually returned to basal levels by 2 h, whereas the expression of *Yy1* increased only moderately. (**b**-**d**) Transcript levels of *Yy1, Egr2, Nab1 and Nab2* in Schwann cells either mock-transfected or transfected with *Yy1*-specific shRNAs and cultured in the absence or presence of NRG1 for 30 min, 1 h or 2 h. The expression of each gene in control cells at time zero was arbitrarily set as 1. (**e**) Luciferase activity measured in NRG1-treated Schwann cells transfected with reporter constructs containing either the *Egr2* promoter or the myelinating Schwann cell enhancer (MSE) of *Egr2*, together with pCX-*Yy1* or empty vector. Values were referred to the readings obtained in untreated cells transfected with empty vector. Error bars, s.d.; **P* < 0.05, ***P* < 0.01.

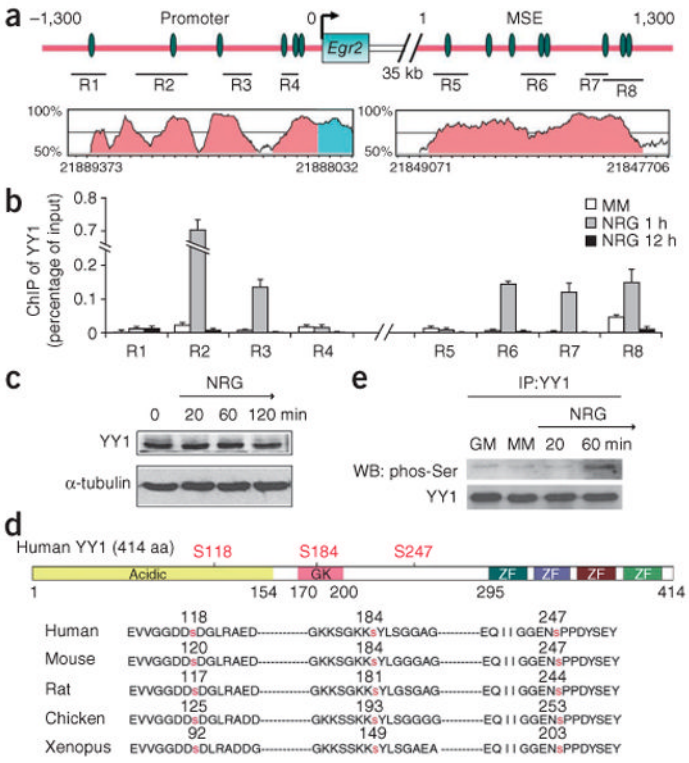

Figure 7.

YY1 binds to chromatin at the *Egr2* locus only in Schwann cells treated with NRG1. (**a**) Schematic diagram of the promoter and MSE of *Egr2*. YY1 consensus binding sequences (green ovals) and the regions (R1–R8) analyzed by chromatin immunoprecipitation are indicated. The plot in pink shows highly conserved sequences between rat and human. Scale marks on *x* axis indicate 50 bp. (**b**) Chromatin from Schwann cells cultured in minimal medium (MM, white bar) or treated with NRG1 for 1 h (gray bars) or 12 h (black bars) was immunoprecipitated (ChIP) with antibodies against YY1 and the regions indicated in **a** were amplified. The results are expressed as percent of input. YY1 was recruited to multiple regions of the *Egr2* promoter and MSE after 1 h NRG1 treatment. (**c**) Protein blot analysis of YY1 in Schwann cells after NRG1 treatment. (**d**) Schematic diagram of human YY1 protein including the acidic N terminus, the glycine-lysine–rich central domain (GK) and the C-terminal DNA-binding domain, which is composed of four zinc fingers (ZF). Three highly conserved serine residues are marked in red. (**e**) Co-immunoprecipitation of protein lysates from rat Schwann cells kept in growth medium (GM) or minimal medium (MM), or treated with NRG1 for 20 min or 1 h. After immunoprecipitation (IP) with anti-YY1 antibodies, the protein blot (WB) was probed with anti-phospho-serine antibodies. Full-length blots are presented in Supplementary Figure 5.

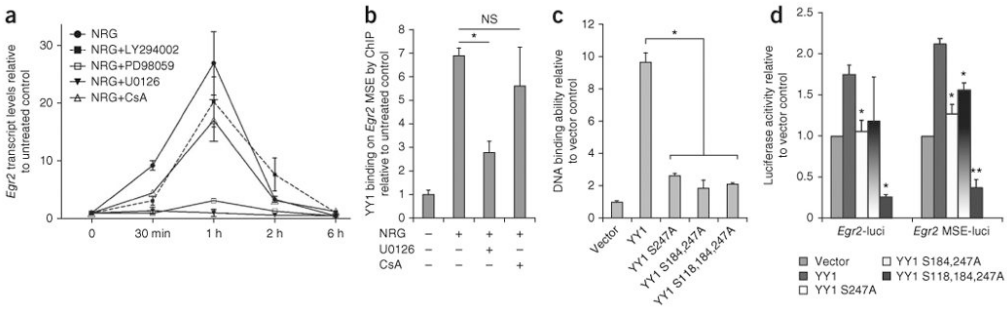

Figure 8.

The regulation of *Egr2* by phosphorylated YY1 is mediated by NRG1-dependent MEK activation. (**a**) Rat Schwann cells were treated with NRG and the PI(3)K inhibitor LY294002, with the MEK inhibitors PD98059 or U0126, or with the calcineurin inhibitor CsA. The transcript levels of *Egr2* were assessed by qRT-PCR. (**b**) ChIP of samples from Schwann cells either untreated or treated with NRG1 alone or with the MEK inhibitor U0126 or the calcineurin inhibitor CsA for 1 h and immunoprecipitated with antibodies to YY1. Note the decreased binding to region 7 of the *Egr2* MSE in cells treated with U0126 but not CsA, in response to NRG stimulation. (**c**) Luciferase assay of Schwann cells cotransfected with YY1 Ser→Ala mutation at position 118, 184, 247 and with Yy1 translucent reporter. Note the decreased ability of mutant YY1 to activate a YY1 binding sequence–driven reporter after NRG treatment. (**d**) Luciferase assay of Schwann cells treated with NRG1 and cotransfected with the indicated reporter constructs and the mutant Yy1 constructs. Error bar, s.d.; **P* < 0.05. ***P* < 0.01.